ЖУРНАЛ СТРУКТУРНОЙ ХИМИИ

2017. Том 58, № 8 *Ноябрь – декабрь* *С. 1706 – 1712*

UDC 548.737:546.562

CRYSTAL STRUCTURE AND MAGNETIC PROPERTIES OF A HYBRID COMPOUND: DISUBSTITUTED BENZYL DIMETHYLAMINOPYRIDINIUM BIS(MALEONITRILEDITHIOLATE)CUPRATE(II)

Y. Liu, Y.-H. Zhou, X.-L. Liao, L.-M. Man, B.-W. Wang, J.-R. Zhou, C.-L. Ni

College of Materials and Energy, Institute of Biomaterial, South China Agricultural University, Guangzhou, P. R. China
E-mail: niclchem@scau.edu.cn (C.-L. Ni)

Received December, 4, 2015

Hybrid compound 1-(2-fluro-4-bromobenzyl)-4-dimethylaminopyridium bis(maleonitriledithiolate)cuprate(II) $[2F4BrBzDMAP]_2[Cu(mnt)_2]$ is prepared and characterized by X-ray diffraction. The compound crystallizes in the triclinic system with the space group *P*-1. The unit cell dimensions are $a = 8.9813(11)$, $b = 9.0794(12)$, $c = 13.1082(17)$ Å and $\alpha = 88.179(2)°$, $\beta = 81.397(2)°$, $\gamma = 70.736(1)°$ with $Z = 1$. The structure consists of two $[2F4BrBzDMAP]^+$ cations and one $[Cu(mnt)_2]^{2-}$ anion. The cations of the title compound stack into a one-dimensional column through p···π and π···π interactions, and the anions (A) and cations (C) are arranged alternatively into one 1D column in an ···A—CC—A—CC—A··· sequence through C—H···N hydrogen bonds and S···N interactions. The presence of functional groups is confirmed by the FT-IR spectrum, and optical absorption is ascertained by the recorded UV-Visible spectrum. The thermal stability of the compound is determined by thermogravimetric and differential thermal analyses. The variable-temperature magnetic susceptibility measurement shows that the compound exhibits a weak ferromagnetic coupling behavior when the temperature is lowered.

DOI: 10.26902/JSC20170824

K e y w o r d s: substituted benzyl dimethylaminopyridium, bis(maleonitriledithiolate) copper(II) anion, weak interactions, magnetic properties.

Hybrid materials containing inorganic complex anions and organic cations have been intensively studied in the past decades owing to their unique molecular configuration, properties and applications, and the study of the design and synthesis of novel hybrid inorganic-organic compounds is a current hot topic in the field of crystal engineering [1, 2]. Transition metal bis(dithiolene) complexes as the significant branches of organic-inorganic hybrid materials have been subjected to the extensive investigation by numerous researchers for their expansive applications in molecular magnets, conductors, and optical devices [3—6]. Over the past few decades, the synthesis and characterization of molecular materials with $[M(mnt)_2]^{n-}$ (M = Ni, Cu, Pt, Co; mnt^{2-} = maleonitriledithiolate, $n = 1$ or 2) complex anions have been received consistent attention due to their square planar structure, delocalized electronic system, and the nature of metal-ligand bonds, and they become potential candidates for the preparation of these original and progressive molecular materials [7—12]. Recently, some molecular solids based on the $[Ni(mnt)_2]^-$ anion and substituted pyridinium organic cations have been widely studied. They display versatile and unusual magnetic properties such as ferromagnetic ordering at low temperatures [13, 14], magnetic transitions from ferromagnetic coupling to diamagnetism [15],

meta-magnetism [16], spin-Peierls-like transitions, and spin-gap system [17, 18]. It has been proven that the introduction of organic cations can change the stacking model of the anions due to some weak interactions such as hydrogen bonds and π···π stacking between these ions. Our laboratory has made much efforts in synthesizing some molecular solids by bringing substituted benzyl 4-dimethylaminopyridium cations into $[Cu(mnt)_2]^{2-}$ anions to establish the contact between the physical properties and crystal structures [19, 20]. In this paper, a molecular solid $[2F4BrBzDMAP]_2[Cu(mnt)_2]$ ($[2F4BrBzDMAP]^+$ = 2-fluro-4-bromobenzyldimethylaminopyridium) is synthesized and illustrated, including the weak interaction such as π···π conjugated effects, *p*···π stacking interactions, as well as C—H···S and C—H···F hydrogen bonds found in the title compound.

EXPERIMENTAL

Synthesis. Commercially available analytical grade materials (2-fluro-4-bromobenzyl bromide, $CuCl_2 \cdot 2H_2O$, and 4-dimethylaminopyridine) were used directly. Disodium maleonitriledithiolate (Na_2mnt) and 1-[2′-fluro-4′-bromobenzyl-4-dimethylaminopyridinium bromide ([2F4BrBzDMAP]Br) were synthesized following the literature procedures [21, 22]. To a Na_2mnt (0.372 g, 2 mmol) solution in methanol (2 ml) a $CuCl_2 \cdot 2H_2O$ (0.171 g, 1 mmol) solution in methanol (10 ml) was slowly added with stirring at ambient temperature. The solution immediately turned to dark red. On continued stirring for 30 min, a [2F4BrBzDMAP]Br (0.782 g, 2 mmol) solution in methanol (20 ml) was dropwise added to the above solution and the precipitated brown solid was filtered and washed with methanol. The mixed solvent of methanol and *iso*-propanol (*v*/*v* = 2:1) of the brown solid was left to evaporate slowly at room temperature. After several weeks of evaporation, the product separated as reddish brown crystals that were isolated by filtration and dried in air. Yield: 81.6 %. Elemental analyses were performed on a model 240 Perkin-Elmer C H N instrument. IR spectra were measured by a Nicolet Avatar 360 FT-IR(range 400—4000 cm^{-1}) spectrophotometer using KBr pellets, and UV-visible spectra were recorded on a SHIMAD20 UV-4000 spectrophotometer. Thermogravimetric analysis (TG/DTA) was carried out on TA Instruments SDT 2960 simultaneous DTA-TGA in a nitrogen stream atmosphere at a heating rate of 10 °C/min^{-1} in the range 50—800 °C. Temperature-dependent magnetic susceptibilities were determined in a field of 2000 Oe and in the range 2.0—300 K on a Quantum Design MPMS-XL SQUID magnetometer. Samples for the magnetic data collection were prepared by finely grinding single crystals into powder and packing the powder into a gelatin capsule. The weight of the sample used for the experiments was 49.26 mg. Correction was made for the background and diamagnetic contributions of the samples according to Pascal′s constants. Anal. Calc. for $C_{36}H_{30}CuN_8S_4F_2Br_2$: C 57.71, H 3.99, N 11.88 %. Found: C 57.65, H 4.07, N 11.76 %.

Single crystal XRD. Reddish brown crystals suitable for the X-ray structure analysis were obtained, and the crystallographic data for the title compound were gathered using graphite-monochromated MoK_α radiation (λ = 0.71073 Å). The structure was solved by direct methods and refined on F^2 by full-matrix least-squares, employing Bruker′s SHELXTL [23]. All non-hydrogen atoms were refined with anisotropic thermal parameters. All H atoms were positioned in the Fourier map and their positions were refined with fixed isotropic thermal parameters. The CIF file with complete information about the structure was deposited with CCDC (No. 1435791), from which it is available free of charge on request at www.ccdc.cam.ac.uk/data_request/cif. Details of the data collection, refinement and crystallographic data are summarized in Table 1.

RESULTS AND DISCUSSION

$[2F4BrBzDMAP]_2[Cu(mnt)_2]$ crystallizes in the triclinic system with the space group *P*-1, and the molecular structure is shown in Fig. 1. There are two $[2F4BrBzDMAP]^+$ cations and one $[Cu(mnt)_2]^{2-}$ anion in a structural unit, and the copper(II) atom in $[Cu(mnt)_2]^{2-}$ anion is the symmetric center of the square plane coordinating two mnt^{2-} anions. Selected bond parameters are listed in Table 2. In one $[Cu(mnt)_2]^{2-}$ anion, the average Cu—S bond distance is 2.273 Å, and the S(1)—Cu(1)—S(2) bond angle within the five-membered ring is 90.93°. These bond parameters and angles are similar to those in

Table 1

Main crystallographic parameters and running characteristics of the X*-ray diffraction experiment for* **1**

Parameter	Value
Empirical formula	$C_{36}H_{30}CuN_8S_4F_2Br_2$
Formula weight	964.28
Wavelength, Å	0.71073
Crystal system; space group	Triclinic; *P*-1
a, *b*, *c*, Å	8.981(2), 9.080(2), 13.108(2)
α, β, γ, deg.	88.179(2), 81.397(2), 70.736(1)
V, Å^3; *Z*	997.5(2); 1
D_c, g/cm^3	1.605
μ, mm^{-1}	2.807
F(000)	483
Crystal size, mm	0.11×0.15×0.21
θ data collection range, deg.	1.57—25.50
Intervals of reflection indices	$-10 \le h \le 10$, $-10 \le k \le 10$, $-15 \le l \le 15$
Measured / Independent reflections	7507 / 3673 [*R*(int) = 0.020]
Completeness, %	99.3
S	1.017
R factors over $I > 2\sigma(I)$	*R*1 = 0.0313, *wR*2 = 0.0966
R factors over all the reflections	*R*1 = 0.0378, *wR*2 = 0.0997
Residual electron density (max / min), e/Å^3	0.43 / –0.59

previously reported $[Cu(mnt)_2]^{2-}$ anions [19, 20]. In the $[2F4BrBzDMAP]^+$ moiety, the dihedral angles between the aromatic rings and the reference plane defined by C(10)—C(11)—N(3) are 95.1° (θ_1) for the pyridine ring, 58.0° (θ_2) for the phenyl ring, while the pyridine and phenyl rings make a dihedral angle of 74.6°(θ_3). The fluorine and bromine atoms are co-planar with the phenyl ring, while the C(17) and C(18) atoms of the dimethylamino group slightly deviate from the pyridine ring with the same deviation of 0.065 Å. The two neighboring cations form a dimer by $p\cdots\pi$ stacking interactions [24] with the distance between N(4) atoms and the centroid of the pyridine ring of 3.846 Å, and the $\pi\cdots\pi$ stacking interactions with a distance of 3.506 Å existing in the phenyl rings of the neighboring dimers result in the formation of a 1D column (Fig. 2, *a*). It is interesting that the $[2F4BrBzDMAP]^+$ cations (C) and $[Cu(mnt)_2]^{2-}$ anions (A) stack alternately into a 1D regular column (Fig. 2, *b*) in an A—CC—A—CC—A sequence through three weak interactions: (1) S···N contacts [25] with a dis-

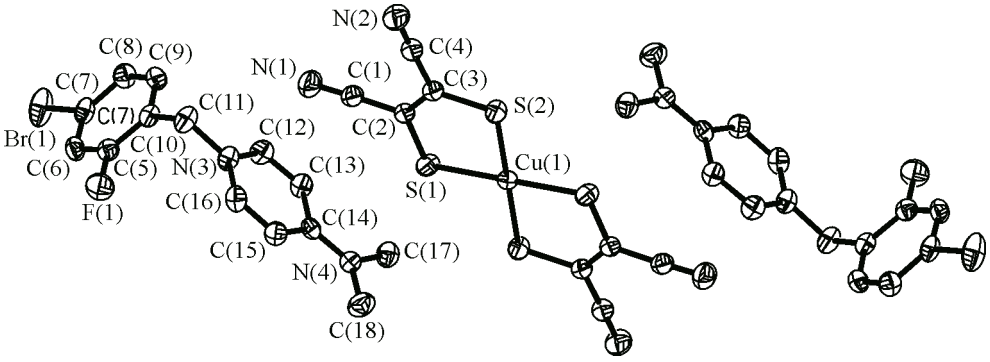

Fig. 1. ORTEP plot (30 % probability ellipsoids) showing the molecular structure of $[2F4BrBzDMAP]_2[Cu(mnt)_2]$

Table 2

Selected bond lengths (*d*, Å) *and bond angles* (ω, deg.) *for* **1**

Bond	*d*	Bond	*d*	Bond	*d*
Cu(1)—S(1)	2.2702(9)	F(1)—C(5)	1.353(3)	N(2)—C(4)	1.150(4)
Cu(1)—S(2)	2.2761(7)	Br(1)—C(7)	1.887(3)	N(3)—C(12)	1.350(4)
S(1)—C(2)	1.733(3)	N(1)—C(1)	1.148(5)	N(4)—C(14)	1.337(4)
S(2)—C(3)	1.742(3)				
Angles	ω	Angles	ω	Angles	ω
S(1)—Cu(1)—S(2)	90.93(3)	Br(1)—C(7)—C(6)	119.2(2)	N(3)—C(11)—C(10)	111.6(2)
S(1)#1—Cu(1)—S(2)	89.07(3)	F(1)—C(5)—C(6)	118.2(2)	N(4)—C(14)—C(13)	122.4(3)
Cu(1)—S(1)—C(2)	101.94(10)	C(11)—N(3)—C(16)	121.5(2)	C(14)—N(4)—C(18)	122.1(3)
Cu(1)—S(2)—C(3)	101.37(9)				

Symmetry transformations used to generate equivalent atoms: #1 *x*+1, *y*, *z*.

tance of 3.600 Å; (2) C(11)—H(11A)···N(1) hydrogen bonds [25] with a C(1A)···N(1) distance of 2.982 Å; (3) the p(N)···π stacking interactions between the pyridine ring of $[2F4BrBzDMAP]^+$ cations and the N atom with a distance of 2.982 Å. All these weak intramolecular interactions offer a great chance in a further generation of a 3D network structure (Fig. 3).

It was observed by comparing the crystal structures of $[2F4BrBzDMAP]_2[Cu(mnt)_2]$ and $[2Br4ClBzDMAP]_2[Cu(mnt)_2]$ that the cell lengths of the former were identical with the those of the latter, while both cell angles were different; the dihedral angles (θ_1, θ_2 and θ_3) in the cation of the former were slightly smaller than those of $[2Br4ClBzDMAP]_2[Cu(mnt)_2]$ [19]. There are C—H···N and S···N weak interactions between the cations and anions of the former, while a short Br···N interaction is found in the latter.

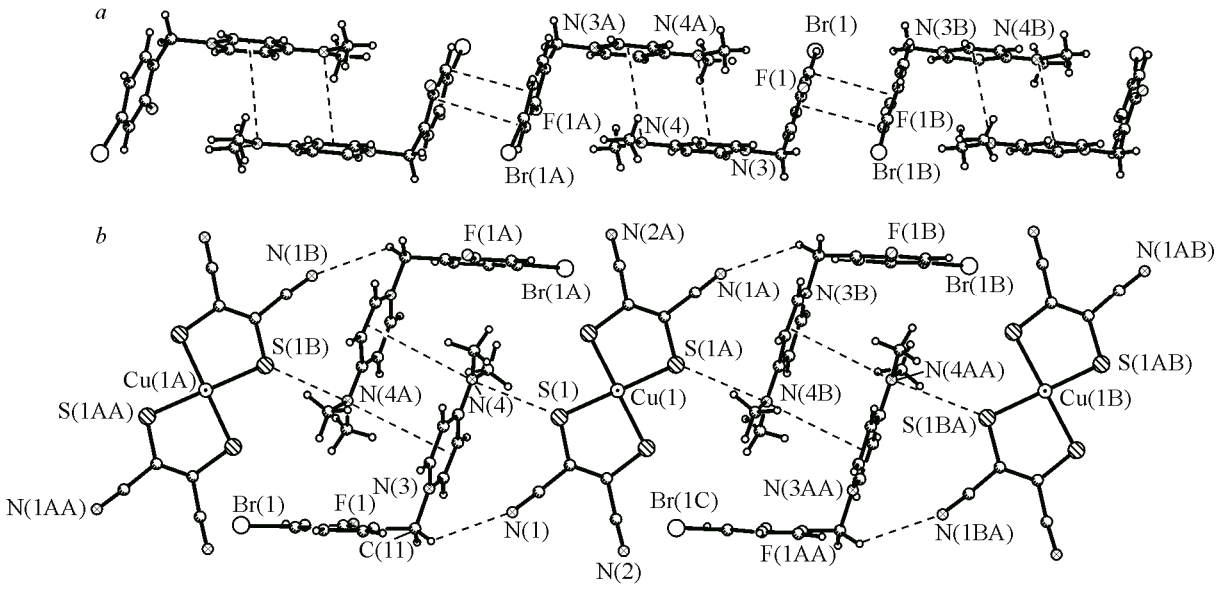

Fig. 2. The one-dimensional column through the *p*···π and π···π stacking interactions between the adjacent $[2F4BrBzDMAP]^+$ cations of $[2F4BrBzDMAP]_2[Cu(mnt)_2]$ (*a*); the C—H···N hydrogen bond and S···N weak interactions between the $[2F4BrBzDMAP]^+$ cations and $[Cu(mnt)_2]^{2-}$ anions of $[2F4BrBzDMAP]_2[Cu(mnt)_2]$ (*b*)

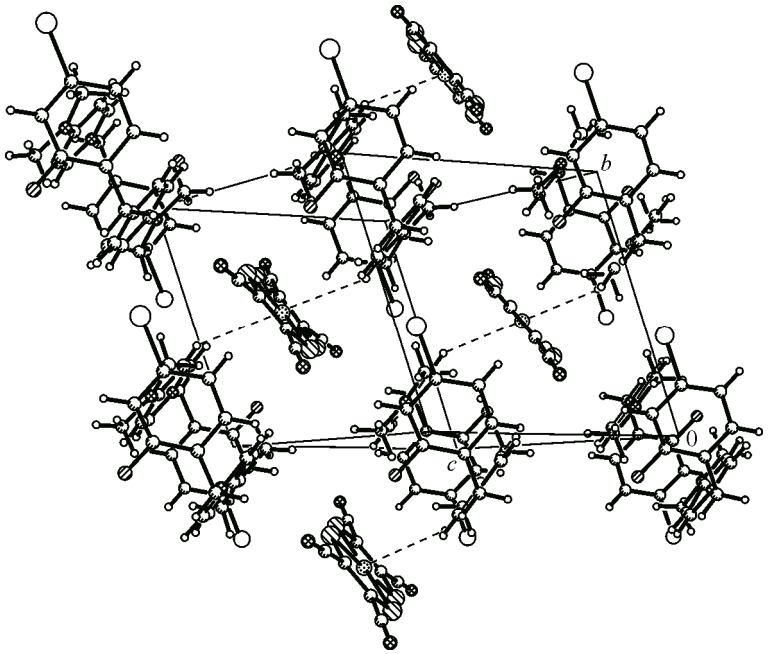

Fig. 3. The packing diagram for $[2F4BrBzDMAP]_2[Cu(mnt)_2]$ as viewed along the *a* axis

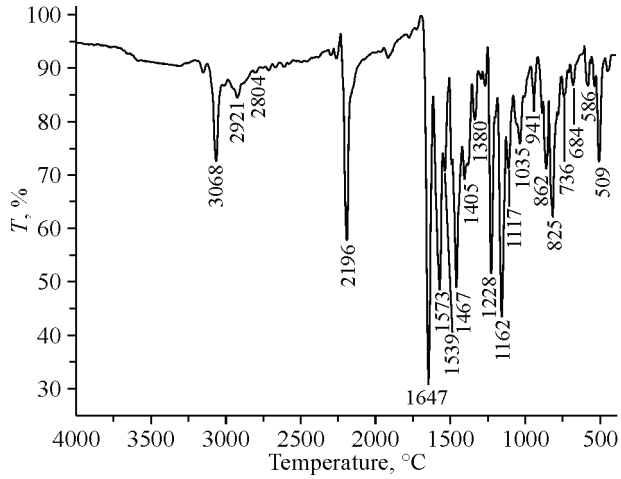

Fig. 4. IR spectra of $[2F4BrBzDMAP]_2[Cu(mnt)_2]$

The IR spectrum is displayed in Fig. 4. The bands at 3068, 2921, and 2804 cm^{-1} are due to the C—H stretching vibrations of the aromatic ring and methylene. The CN stretching band lies at 2194 cm^{-1} from mnt^{2-} ligands. The bands at 1647 cm^{-1} are attributable to the (C=C) stretching bands of the aromatic rings. The C=C stretching band from the mnt^{2-} ligand is at 1467 cm^{-1} [26]. The C—F stretching band lies at 1162 cm^{-1}, meanwhile, the C—Br stretching band is observed at 509 cm^{-1}. The bond at 862 cm^{-1} is alleged as the C—H bending vibration of the phenyl ring.

The UV-vis absorption spectra of $[2F4BrBzDMAP]_2[Cu(mnt)_2]$ in CH_3CN are shown in Fig. 5. The characteristic bands at 479, 371 cm^{-1}, and 288 nm are assigned to $M \rightarrow L$, $L(\pi) \rightarrow M$, and $L^* \rightarrow L$ respectively, which are basically similar to those observed in $[2Br4ClBzDMAP]_2[Cu(mnt)_2]$ [19].

TG and DTA of $[2F4BrBzDMAP]_2[Cu(mnt)_2]$ were recorded at a heating rate of 10 °C/min^{-1} in the range from 50 to 800 °C within the test illustrated in Fig. 6. In the DTA curve, the spiky endo-

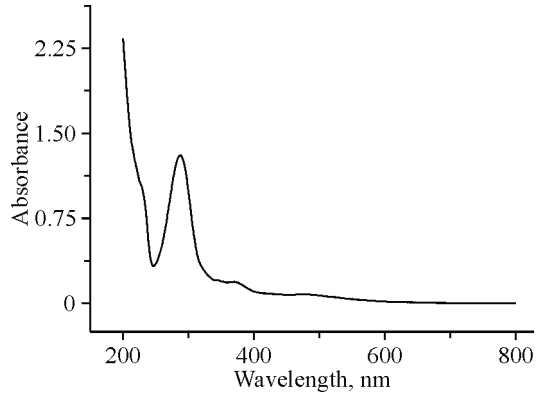

Fig. 5. UV-Vis absorption spectra of $[2F4BrBzDMAP]_2[Cu(mnt)_2]$

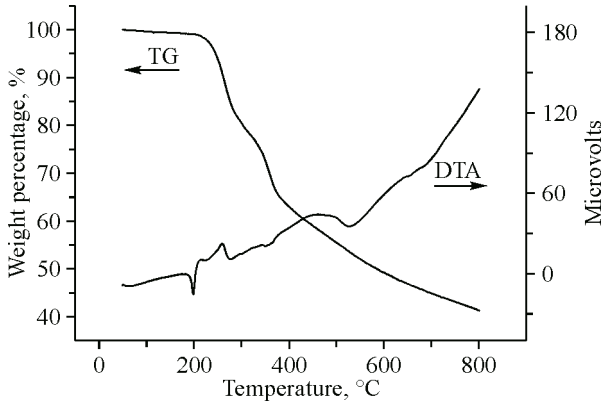

Fig. 6. TG-DTA thermal curves of $[2F4BrBzDMAP]_2[Cu(mnt)_2]$

thermic peak is observed at 198.50 °C, corresponding to the melting point of the material, and it also reveals the sample purity and high crystallinity. It can be observed in Fig. 6 that the reversible endothermic transition arises at 258.70 °C, which is attributed to volatilization of the sample. The TG curve exhibits that the complex decomposes in two stages of the weight loss [26]. The TG curve of the compound reveals that it is stable up to 198.50 °C. The first step in the weight loss of the title compound occurs at 226.31—277.97 °C (experimental value is 13.53 %), which corresponds to the loss of CS_2 and CS. On continued heating of metal sulfide, the second step weight loss appeared at 277.97—375.58 °C, and the experimental value is 18.60 %, which caused the formation of metal nitride. On continued heating, the compound further disintegrates and the total experimental mass loss is 58.70 %.

Magnetic properties. $[2F4BrBzDMAP]_2[Cu(mnt)_2]$ exhibits a weak ferromagnetic exchange interaction. As shown in Fig. 7, *a*, the $\chi_m T$ value increased slowly from 0.379 emu·K/mol^{-1} at 300 K to 0.538 emu·K/mol^{-1} at 12 K, and increased abruptly to 0.671 emu·K/mol^{-1} at 2 K. The best fit formula (the red solid line in Fig. 7, *a*) for the temperature-dependent magnetic susceptibility in the temperature range 2—300 K, according to the Curie-Weiss law, gives $C = 0.376$ emu·K/mol^{-1}, $\theta = 0.856$ K, and $R = 1.2\times10^{-5}$ (R is the agreement factor defined as $\sum(\chi_M^{calcd} - \chi_M^{obsd})^2 / (\chi_M^{obsd})^2$). The weak ferromagnetic coupling behavior is confirmed by the dependence of isothermal magnetization at 2 K (Fig. 7, *b*), and the red solid line from the Brillouin function ($s = 1/2$, $g = 2.00$). The magnetization increases very rapidly before the field reaches 10 kOe, above which the magnetization saturates rapidly with increasing field. The saturation magnetization is 5632 emu·G/mol^{-1}, which is slightly larger

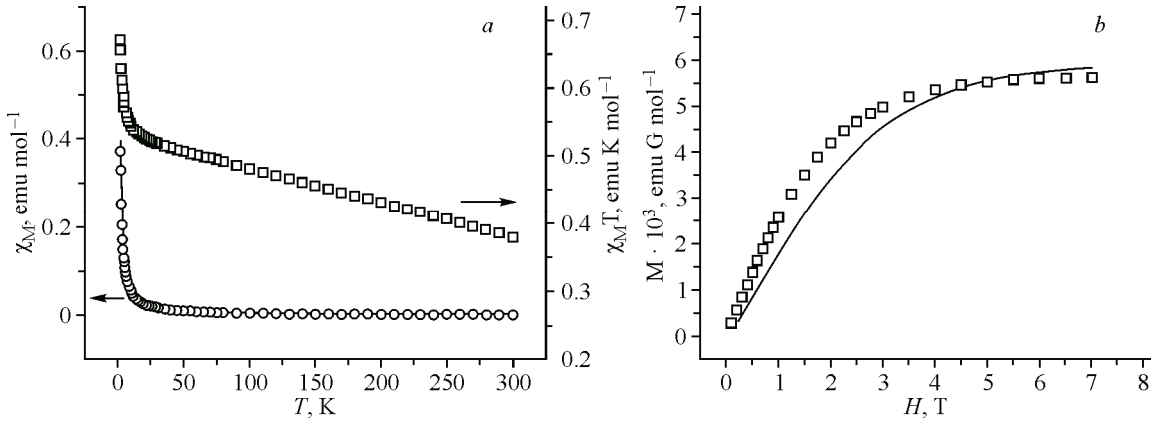

Fig. 7. Plots of χ_M and χ_M^{-1} vs T for $[2F4BrBzDMAP]_2[Cu(mnt)_2]$ (*a*); plot of M vs H of $[2F4BrBzDMAP]_2[Cu(mnt)_2]$ (the red solid line from the Brillouin function) (*b*)

than the saturation value (5585 emu·G/mol^{-1}) expected for Cu(II) species. The magnetic coupling between $[Cu(mnt)_2]^{2-}$ anions is very sensitive to the overlap fashion of the neighboring $[Cu(mnt)_2]^{2-}$ anions and intermolecular weak interactions [19, 20]. The magnetic property of the title compound different from that of $[2Br4ClBzDMAP]_2[Cu(mnt)_2]$ [19] is due their structural difference. When the 4-substituted group in the benzyl ring is a Br atom and the 2-substituted group was changed from H to the F atom, the similarities in the stacking mode of the ions and weak interactions are responsible for the magnetic similarities of $[4BrBzDMAP]_2[Cu(mnt)_2]$ [20] and $[2F4BrBzDMAP]_2[Cu(mnt)_2]$.

This research was supported by the Science and Technology Project (No. 2014A010105037) from Guangdong Science and Technology Department, and the university students′ innovative training project (No. 201410564195) from the Education Department of Guangdong Province.

REFERENCES

1. *Sanchez C., Belleville P., Popall M., Nicole L.* // Chem. Soc. Rev. – 2011. – **40**, N 2. – P. 696.
2. *Vallet-Regi M., Colilla M., Gonzalez B.* // Chem. Soc. Rev. – 2011. – **40**, N 2. – P. 596.
3. *Duan H.B., Ren X.M., Meng Q.J.* // Coord. Chem. Rev. – 2010. – **254**, N 13-14. – P. 1509.
4. *Karakas I.A., Iliopoulos K., El-Ghayoury B., Derkowska-Zielinska A., Ranganathan A., Batail P., Migalska-Zalas A., Sahraouil B., Karakaya M.* // Opt. Mater. – 2013. – **36**, N 1. – P. 106.
5. *Coomber A.T., Beljonne D., Friend R.H., Brédas J.L., Charlton A., Robertson N., Underhill A.E., Kurmoo M., Day P.* // Nature. – 1996. – **380**. – P. 144.
6. *Bruce A.K., Michael J.F., Pamela J.S.* // Inorg. Chem. – 2008. – **47**. – P. 5696.
7. *Zarkadoulas A., Koutsouri E., Christina K., Mitsopoulou C.A.* // Coord. Chem. Rev. – 2012. – **256**, N 21-22. – P. 2424.
8. *Robertson N., Cronin L.* // Coord. Chem. Rev. – 2002. – **227**, N 1. – P. 93.
9. *Wilkinson G., Gillard R.D., McCleverty J.A.* // Comprehensive Coord. Chem. – New York, 1987.
10. *Kishore R., Tripuramallu B.K., Durgaprasad G., Das S.K.* // J. Mol. Struct. – 2011. – **990**, N 1-3. – P. 37 – 43.
11. *Mochida T., Funasako Y., Kishida T., Terajima C.K.* // Inorg. Chim. Acta. – 2012. – **384**, N 1. – P. 111.
12. *Urichi M., Yakushi K., Yamashita Y., Qin J.* // J. Mater. Chem. – 1998. – **8**, N 2. – P. 141.
13. *Xie J.L., Ren X.M., Song Y., Zhou Y., Meng Q.J.* // J. Chem. Soc., Dalton Trans. – 2002. – P. 2868.
14. *Xie J.L., Ren X.M., Song Y., Zhang W.W., Liu W.L., He C., Meng Q.J.* // Chem. Commun. – 2002. – **20**. – P. 2346.
15. *Xie J.L., Ren X.M., Gao S., Zhang W.W., Li Y.Z., Lu C.S., Ni C.L., Liu W.L., Meng Q.J., Yao Y.G.* // Eur. J. Inorg. Chem. – 2003. – **14**. – P. 2393.
16. *Ni C.L., Dang D.B., Li Y.Z., Song Y., Ni Z.P., Tian Z.F., Yuan Z.R., Gao S., Meng Q.J.* // Solid State Sci. – 2006. – **8**, N 5. – P. 520.
17. *Ren X.M., Meng Q.J., Song Y., Lu C.S., Hu C.J., Chen X.Y., Xue Z.L.* // Inorg. Chem. – 2002. – **41**, N 23. – P. 5931.
18. *Hu Y.L., Lin J.H., Han S., Chen W.Q., Yu L.L., Zhou D.D., Yin W.T., Zuo H.R., Zhou J.R., Yang L.M., Ni C.L.* // Synth. Met. – 2012. – **162**. – P. 1024.
19. *Huang Q., Lin J.H., Liang L.B., Chen X., Zuo H.R., Yang L.M., Ni C.L., Hu X.L.* // Inorg. Chim. Acta. – 2010. – **363**, N 11. – P. 2546.
20. *Davison A., Holm R.H.* // Inorg. Synth. – 1967. – **10**, N 2. – P. 8.
21. *Bulgarevich S.B., Bren D.V., Movshovic D.Y., Finocchiaro P., Failla S.* // J. Mol. Struct. – 1994. – **317**, N 1-2. – P. 147.
22. *Sheldrick G.M.* SHELXTL, Structure Determination Software Programs, Version 5.10. Bruker Analytical X-ray Systems Inc. – Madison, Wisconsin, USA, 1997.
23. *Das A., Choudhury S.R., Dey B., Yalamanchili S.K., Helliwell M., Gamez P., Mukhopadhyay S., Estarellas C., Frontera A.* // J. Phys. Chem. B. – 2010. – **114**, N 15. – P. 4998.
24. *Pham P.T.T., Bader M.M.* // Cryst. Growth. Des. – 2014. – **14**, N 3. – P. 916.
25. *Johnson M.K.* Vibrational spectra of dithiolene complexes in dithiolenechemistry, progress in inorganic chemistry. – Widely, New York, 2004.
26. *Prasad R., Kumar A.* // Thermochim. Acta. – 2002. – **383**, N 1-2. – P. 59.